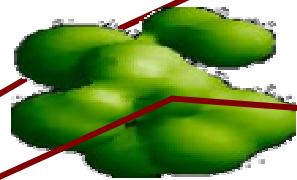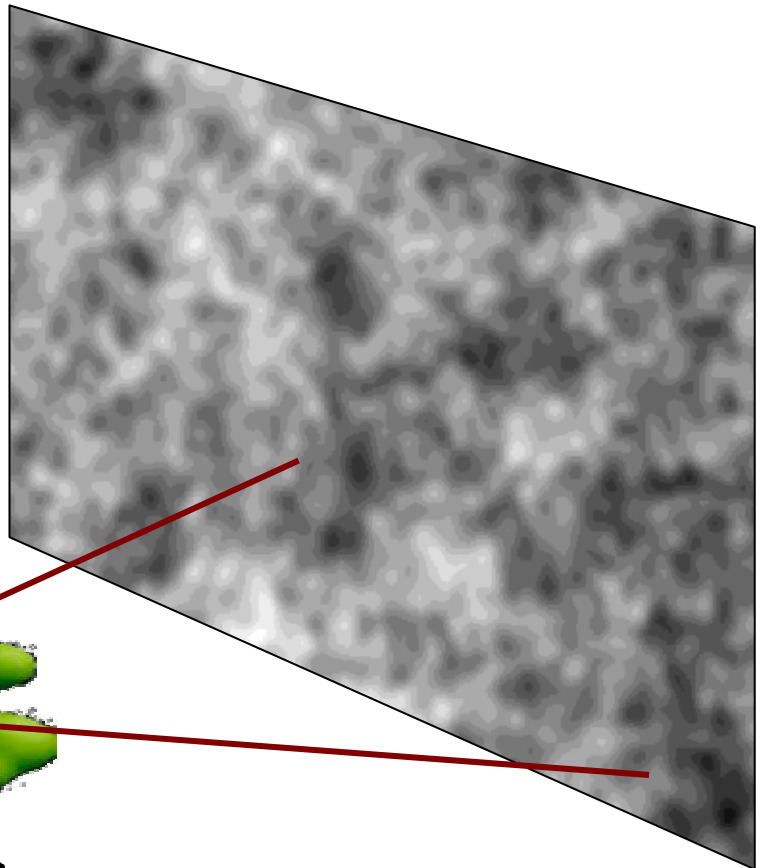*Francis Bernardeau*
SPhT Saclay

Lensing on CMB and its correlation with LSS surveys

Lensing effects, one of the (many) secondary effects

- ISW effects in linear and nonlinear regimes
- SZ effects
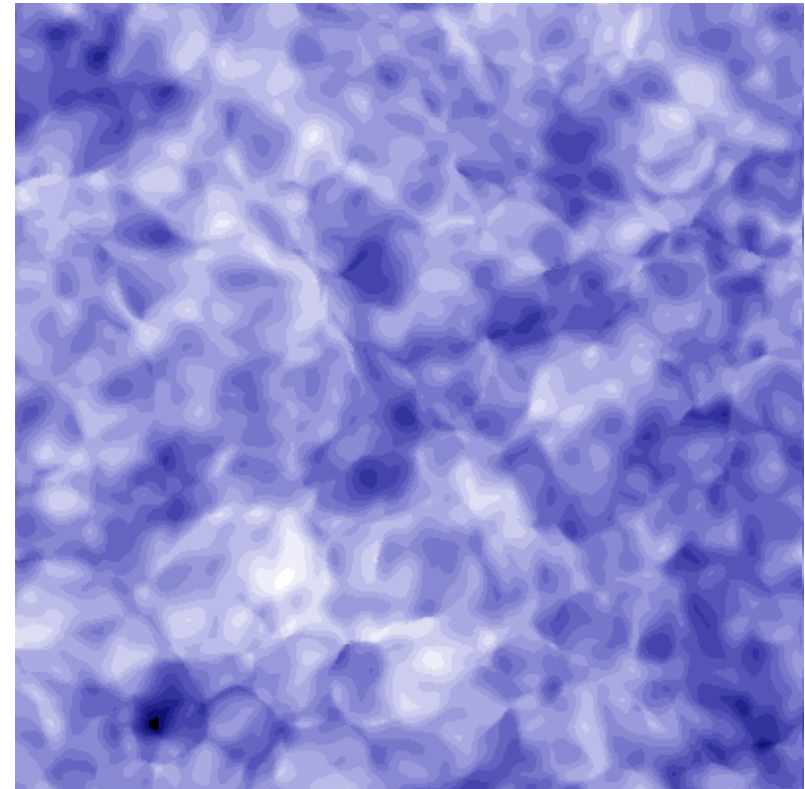- Lensing effects

Intervening potential well

Lenses on CMB

- The principle

$$\hat{T}(\vec{\alpha}) = T\left(\vec{\alpha} + \vec{\xi}\right)$$

displacement field

$$\xi(\gamma) = \int_0^{\chi_{\mathrm{CMB}}} \mathrm{d}\chi \; w(\chi) \int \frac{\mathrm{d}^3 k}{(2\pi)^{3/2}} \times$$

$$\frac{i\,k_\perp}{k^2\,\mathcal{D}(\chi)} \; \delta(k) \; \exp\left[i\mathcal{D}(\chi)\,k_\perp \cdot \gamma + i k_r\,\chi\right].$$

$$w(\chi) = \frac{3\Omega_0}{a(\chi)} \frac{\mathcal{D}(\chi_{\mathrm{CMB}} - \chi)\,\mathcal{D}(\chi)}{\mathcal{D}(\chi_{\mathrm{CMB}})}.$$
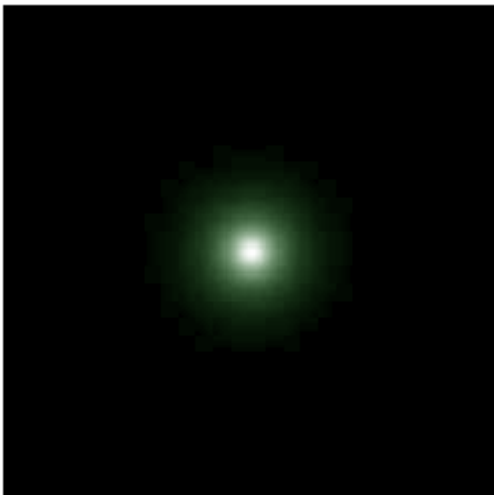
- Large scale mode couplings
- Extra small scale power
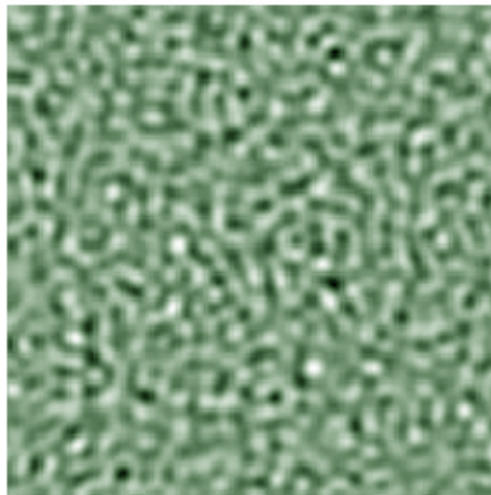
On the polarization

- Similar effects on the polarization
  components

$$\hat{Q}(\vec{\alpha}) = Q(\vec{\alpha} + \vec{\xi}), \qquad \hat{U}(\vec{\alpha}) = U(\vec{\alpha} + \vec{\xi}).$$

$$\Delta \hat{E} = \Delta E + \xi^i \partial_i \Delta E - 2\kappa \Delta E - 2\delta_{ij} \left(\gamma^i \Delta P^j + \gamma^i_{,k} P^{j,k} \right)$$

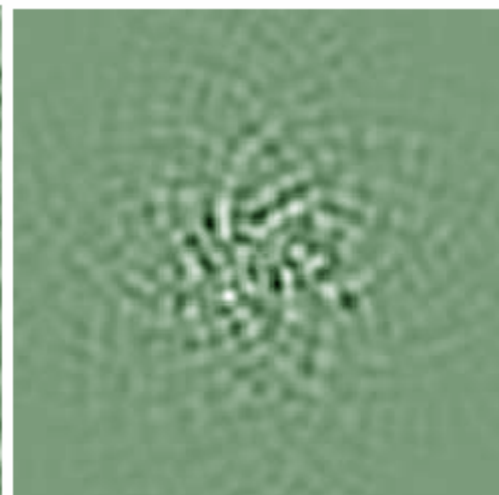$$\Delta \hat{B} = \qquad\qquad -2\epsilon_{ij} \left(\gamma^i \Delta P^j + \gamma^i_{,k} P^{j,k} \right)$$

The Lens   The E field   and the B field

Consequences (1)

- Mode couplings that induce specific higher order correlation functions (FB '97 + …)

- Possibilities of reconstructing the lens power spectrum from CMB temperature and polarization

  (Zaldarriaga & Seljak '99 + …)

Lenses on CMB: intrinsic effects

- Temperature 4-pt correlation function
- Temperature tri-spectrum *(Hu '01)*
- Measuring the convergence power spectrum from T and B observations
  - Mathematically impossible to deconvolve B and get the convergence field (from one given realization), Benabed et al. '00
  - Optimal reconstruction schemes when CMB is viewed as a source plane covered with random structures (e.g. a cosmic shear approach)

Trispectrum and 4-pt function

- The tri-spectrum in the small angle approximation

$$\delta\hat{T}_l = \delta T_l + \frac{\mathbf{l}_1.\mathbf{l}_2}{l_2^{\,2}}\,\delta T_{l_1} * \kappa_{l_2} + \ldots$$

$$\left\langle \delta T(\mathbf{l}_1)\delta T(\mathbf{l}_2)\delta T(\mathbf{l}_3)\delta T(\mathbf{l}_4)\right\rangle_c = \delta_{Dirac}(\mathbf{l}_1 + \mathbf{l}_2 + \mathbf{l}_3 + \mathbf{l}_4)C(l_1)C(l_2)$$

$$\int_{Obs.}^{CMB} d\chi \frac{\mathbf{l}_1.\mathbf{l}_3}{l_3^{\,2}}\frac{\mathbf{l}_2.\mathbf{l}_3}{l_3^{\,2}} P_{matter}\left(\frac{l_3}{D}\right)w(D, D_{CMB}) + perm.$$
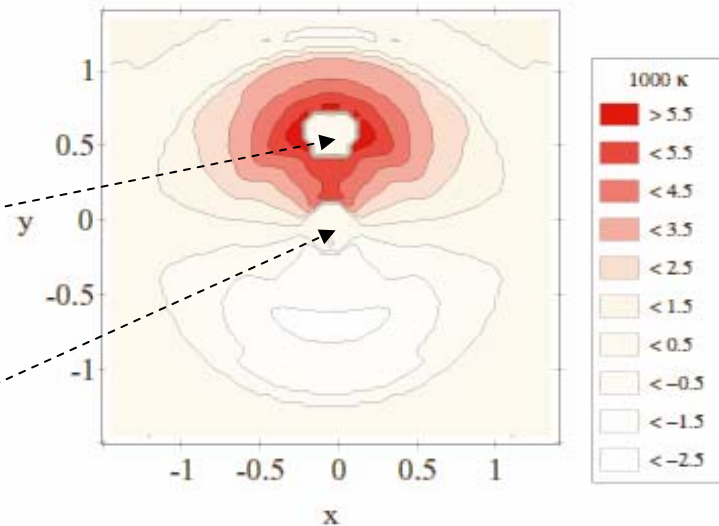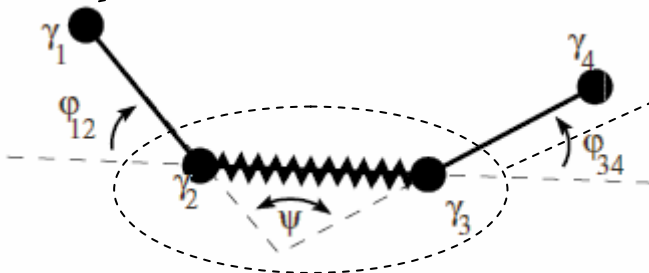
- The 4-point function

Fig. 6. Contour plot of the function $\kappa_4(\gamma_{12}, \gamma_{23})$ (eq. 29) as a function of the relative position (in degrees) of γ_3 when γ_2 is the central point of the graph and γ_1 is at the coordinates $x = 0$, $y = +0.63$ deg. The value of κ_4 has been multiplied by 1000.

Other statistical effects

- Hot spot correlation function

  » *Takada et al. '00*

- Temperature ellipticity statistics, cumulants

  » *Bernardeau '99, Kesden et al. '02*

- Genus and Minkowski functionnals

  » *Schmalzing et al. '00, Takada '01*

- …

Reconstructing the convergence power spectrum

Hirata & Seljak '03, Hu & Okamoto '02,
Kesden, Cooray & Kamionkowski '03

- Correlation functions give the Fourier modes of the potential to a kernel function,

$$\langle x(\mathbf{l})x'(\mathbf{l}')\rangle_{CMB} = f_\alpha(\mathbf{l},\mathbf{l}')\phi(\mathbf{L})$$

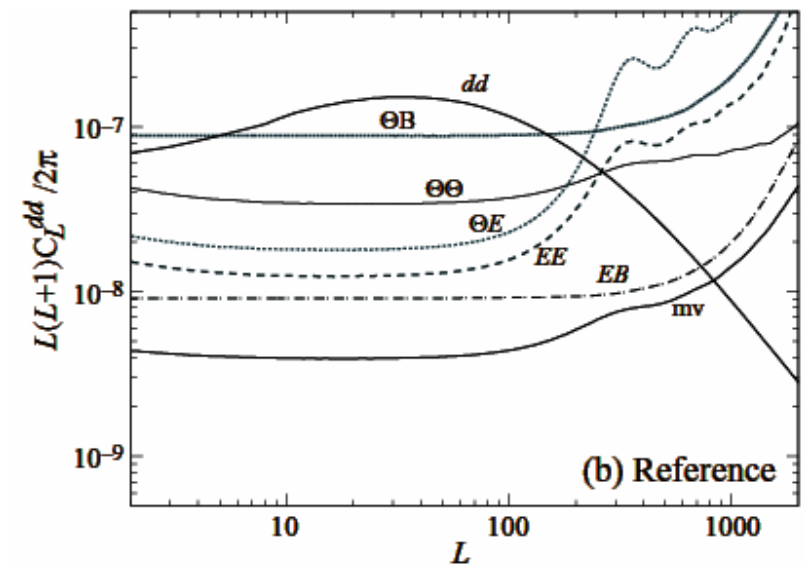| α	$f_\alpha(\mathbf{l}_1,\mathbf{l}_2)$
$\Theta\Theta$	$\tilde{C}_{l_1}^{\Theta\Theta}(\mathbf{L}\cdot\mathbf{l}_1) + \tilde{C}_{l_2}^{\Theta\Theta}(\mathbf{L}\cdot\mathbf{l}_2)$
ΘE	$\tilde{C}_{l_1}^{\Theta E}\cos\varphi_{\mathbf{l}_1\mathbf{l}_2}(\mathbf{L}\cdot\mathbf{l}_1) + \tilde{C}_{l_2}^{\Theta E}(\mathbf{L}\cdot\mathbf{l}_2)$
ΘB	$\tilde{C}_{l_1}^{\Theta E}\sin 2\varphi_{\mathbf{l}_1\mathbf{l}_2}(\mathbf{L}\cdot\mathbf{l}_1)$
EE	$[\tilde{C}_{l_1}^{EE}(\mathbf{L}\cdot\mathbf{l}_1) + \tilde{C}_{l_2}^{EE}(\mathbf{L}\cdot\mathbf{l}_2)]\cos 2\varphi_{\mathbf{l}_1\mathbf{l}_2}$
EB	$[\tilde{C}_{l_1}^{EE}(\mathbf{L}\cdot\mathbf{l}_1) - \tilde{C}_{l_2}^{BB}(\mathbf{L}\cdot\mathbf{l}_2)]\sin 2\varphi_{\mathbf{l}_1\mathbf{l}_2}$
BB	$[\tilde{C}_{l_1}^{BB}(\mathbf{L}\cdot\mathbf{l}_1) + \tilde{C}_{l_2}^{BB}(\mathbf{L}\cdot\mathbf{l}_2)]\cos 2\varphi_{\mathbf{l}_1\mathbf{l}_2}$

FIG. 3.— Deflection signal (*dd*) and noise power spectra of the quadratic estimators and their minimum variance (mv) combination: (a) Planck experiment (b) reference experiment. As the sensitivity of the experiment improves the best quadratic estimator switches from $\Theta\Theta$ to EB. Only the EB-estimator can reconstruct the mass distribution at $L \gtrsim 200$.

<10>

The reconstructed power spectrum,

Hu & Okamoto '02

Reference experiment:
a nearly perfect
experiment with a
noise level of $\Delta T =$
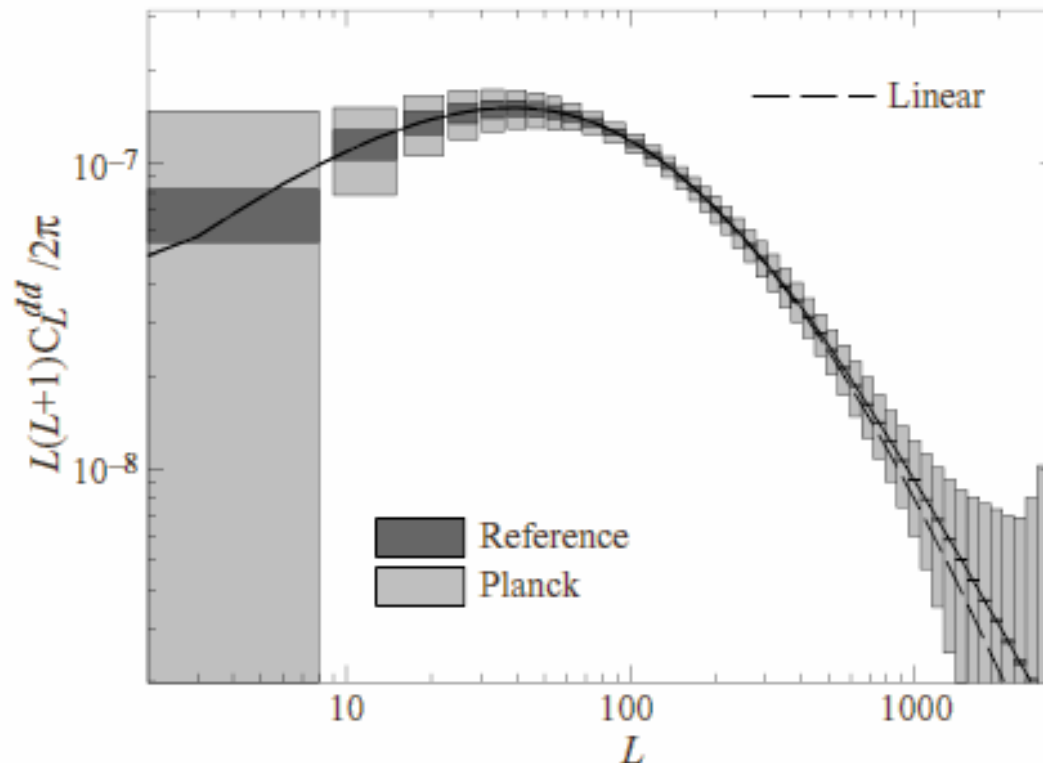$\Delta P/\sqrt{2} = 1\mu K$-arcmin
and a beam of $= 4'$

FIG. 6.— Statistical errors achievable on the deflection power spectrum with the Planck ($f_{sky} = 0.65$) and reference experiments ($f_{sky} = 1$). Boxes represent band averaging width and 1σ errors. The polarization information in the reference experiment allows for a cosmic variance limited measurement of the projected power spectrum out to $L \sim 1000$. In this regime, the fluctuations are almost completely linear (dashed lines).

Reconstructing the convergence maps, *Hirata & Seljak '03*
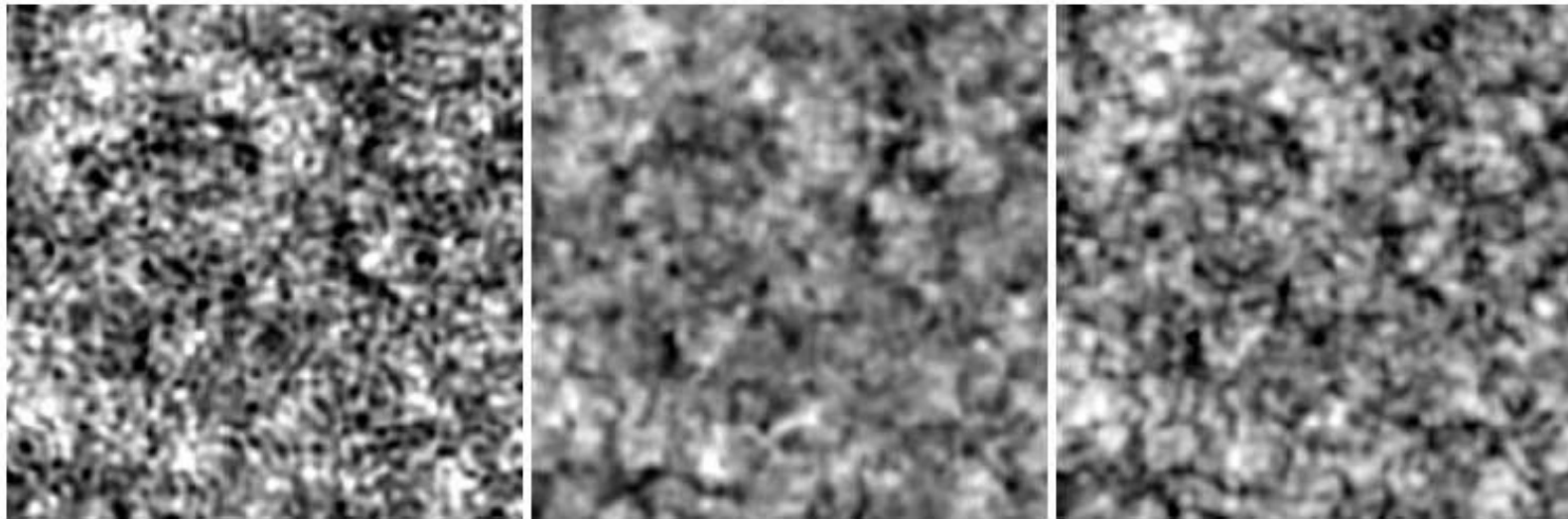
Quadratic estimators

Maximum likelihood

FIG. 4: A simulated reconstruction of the lensing convergence using polarization and Reference Expt. C parameters. In the left panel, we display the realization of the convergence field κ used to produce the simulated CMB. The reconstructions using the Wiener-filtered quadratic estimator and the iterative estimator are shown in the center and right panels, respectively. These frames are each $8°\,32'$ in angular width, corresponding to 1/16 of the simulated area; the scale ranges from black (diverging, $\kappa = -0.12$) through white (converging, $\kappa = +0.12$). Although all lensing multipoles up to $l = 3600$ are simulated, we have only displayed the $l \leq 1600$ modes in these figures for clarity. Field rotation was neglected in the calculations for this figure.

Consequences (2)

- Expected correlations with local surveys that share a fair amount of potential wells : CMB-LSS correlations
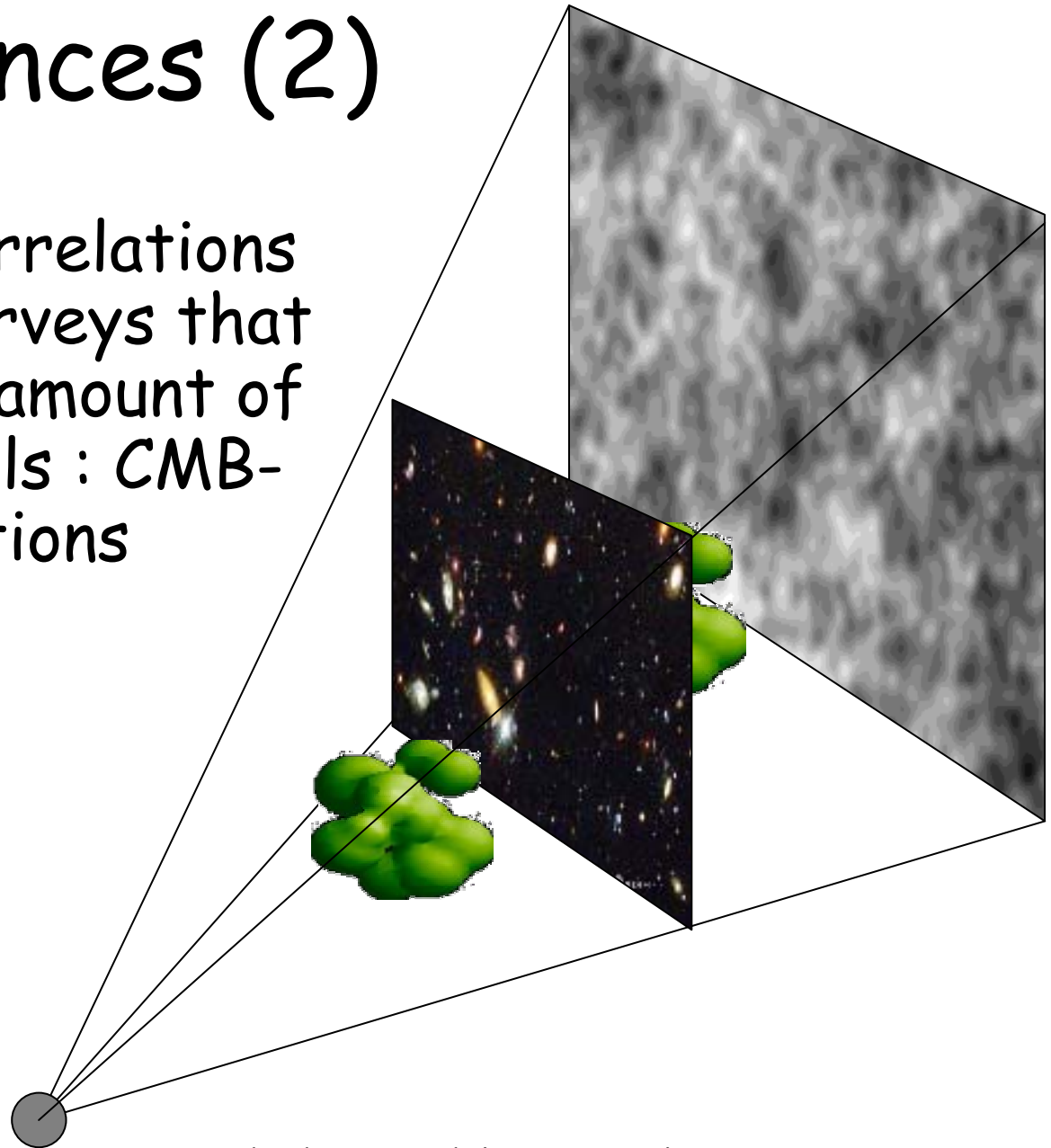
CMB LSS correlations

- How many haloes are in common?

$$r(z_{\text{gal}}) = \frac{\langle \kappa\, \kappa_{\text{gal}} \rangle}{\sqrt{\langle \kappa^2 \rangle \langle \kappa_{\text{gal}}^2 \rangle}}$$

	$z_{\text{gal}} = 1$	$z_{\text{gal}} = 2$
r coefficient	0.42	0.60
EdS, Linear	0.31	0.50
$\Omega = 0.3$, $\Lambda = 0.7$, Linear	0.40	0.59
$\Omega = 0.3$, $\Lambda = 0.7$, Non Linear		

TABLE I. values of r, the cross-correlation between two source planes (z_{gal} and $z_{\text{emb}} = 1100$) for different models. The adopted filter scale (see Sect. III C for details) is 2 arcmin for both weak lensing survey and Cosmic Microwave Background observations. Non-linear $P(k)$ has been computed using Peacock and Doddsmethod [17].

- Detecting CMB LSS correlations
  - Through temperature field
  - Through polarization field

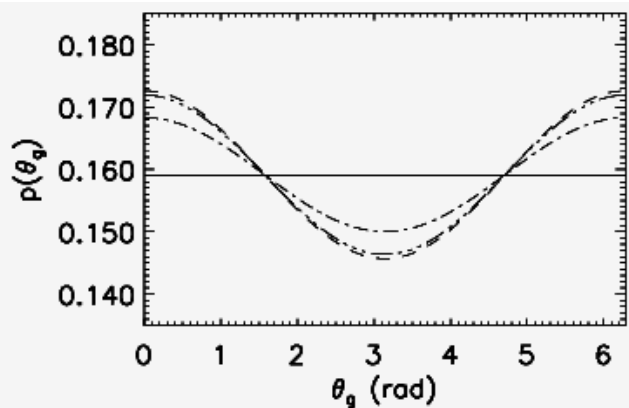# CMB temperature – LSS correlations *van Waerbeke et al. '00*

- To see the temperature field as a distorted source plane with Gaussian fluctuations

- Local ellipticity parameter

$$\mathbf{e} = \left(\frac{\partial_x^2 \delta_T - \partial_y^2 \delta_T}{\partial_x^2 \delta_T + \partial_y^2 \delta_T} ; \frac{2\partial_{xy}\delta_T}{\partial_x^2 \delta_T + \partial_y^2 \delta_T} \right)$$

- … correlated with galaxy ellipticities

$$\cos(\theta_g) = \frac{\hat{\mathbf{e}} \cdot \gamma_g}{\hat{e}\gamma_g}$$

$$\mathcal{P}(\theta_g)\mathrm{d}\theta_g = \frac{\mathrm{d}\theta_g}{2\pi}\left(1 + 3\sqrt{\frac{\pi}{2}} \frac{\langle \kappa\kappa_g \rangle}{\langle \kappa_g^2 \rangle^{1/2}} \cos(\theta_g) \right)$$
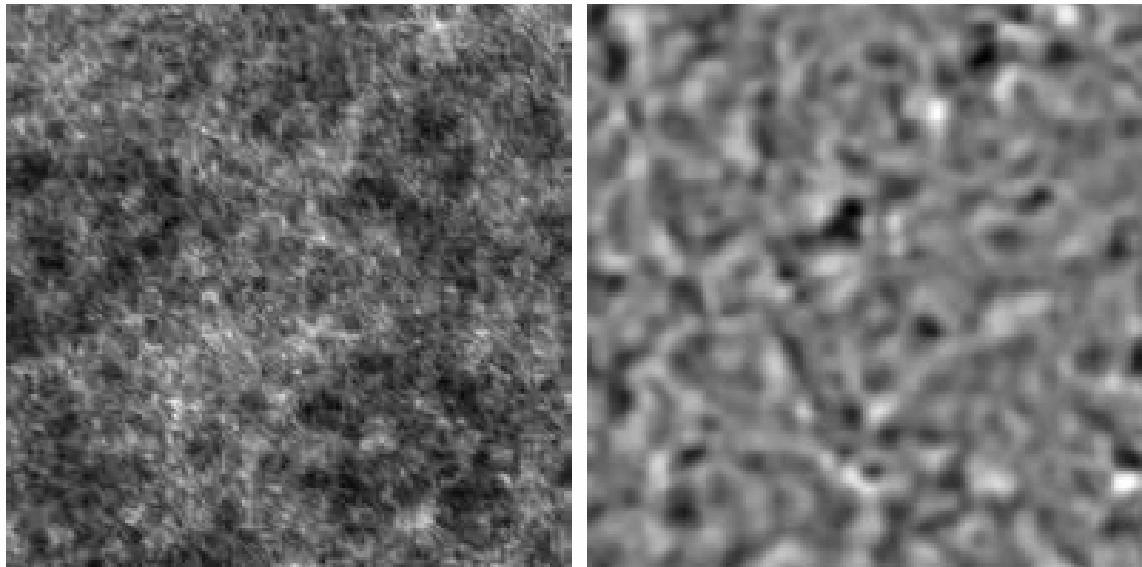

VALUES OF $\langle \cos(\theta_g) \rangle$ AND ITS SIGNAL-TO-NOISE

	$\langle \cos(\theta_g) \rangle$ for $\theta_0 = 5'$	S/N for $\theta_0 = 2.5'$	S/N for $\theta_0 = 5'$	S/N for $\theta_0 = 10'$
standard-CDM (900 deg^2)	0.057	8.3	5.4	3.3
Λ-CDM (900 deg^2)	0.054	10.7	6.7	3.9
Open-CDM (900 deg^2)	0.040	7.5	4.4	2.3

CMB Polarization - LSS correlations

- Given what we know the expected ΔB field is

  Benabed et al. '00

  $$b = \epsilon_{ij} \left(\gamma_{\text{gal}}^i \Delta \hat{P}^j + \gamma_{\text{gal,k}}^i \hat{P}^{j,k} \right)$$

- – It gives an expected signal with cosmic variance = 2 to 5 % for 100 □²

<16>

The CMB LSS cross-spectra

Hu & Okamoto '02

• It is always possible to correlate convergence reconstructed field and galaxy convergence fields

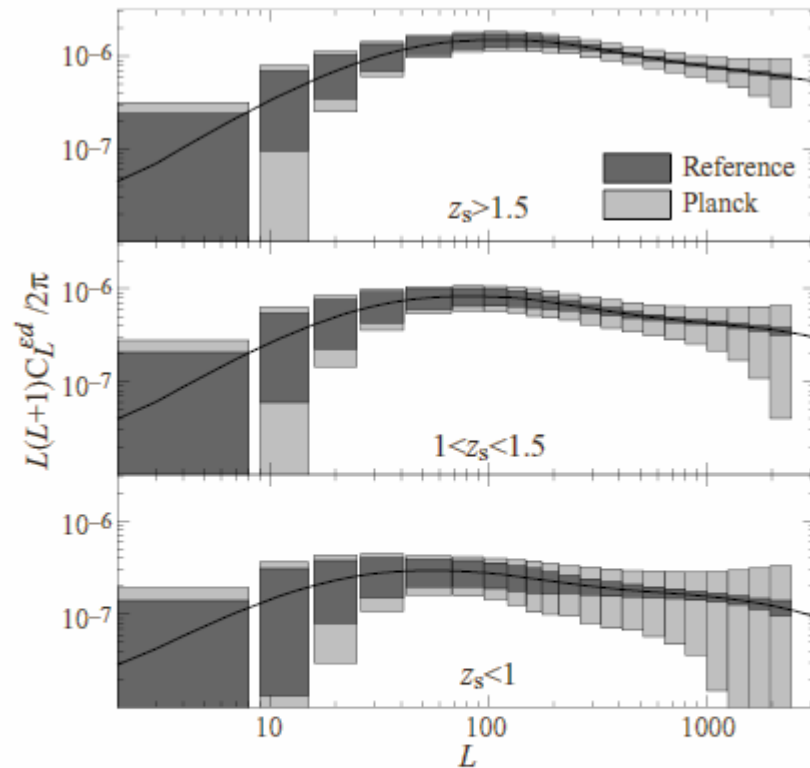 • CMB-cosmic shear correlations for different source planes

FIG. 7.— Statistical errors on the cross correlation of CMB deflections and cosmic shear in three source redshift bands on a 1000 deg^2 patch of sky for the Planck and reference experiment. Assumptions for the cosmic shear experiment are given in the text. Precision measurements from the polarization estimators enables highly significant cross correlation detection and hence tomographic studies of structure evolution.

What would we learn ?

- Constraints on cosmological parameters
- Constraints on the dark energy equation of state from the NL power spectrum
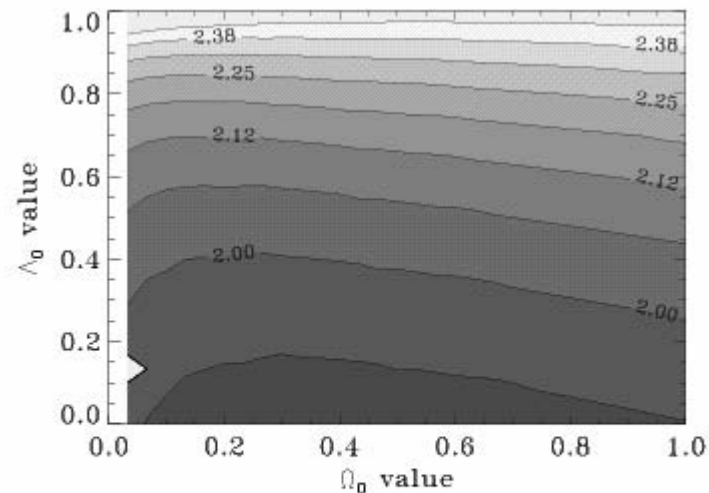- Test of large-scale gravity

FIG. 5. $\left\langle \kappa_{(\theta)} \kappa_{gal(\theta_{gal})} \right\rangle / \left\langle \kappa^2_{gal(\theta_{gal})} \right\rangle$ for a CDM model consistent with the values of (Ω_0, Λ). $\theta = \theta_{gal} = 2'$.

Further consequences

- Any tracer of the large-scale structure is bound to be correlated with CMB anisotropies and polarization
  - Large–scale structure is traced by dusty star–forming galaxies, that also induce anisotropies in the far–infrared background (FIRB), *Song et al. 02.*

<19>

Remarks

- Other possible CMB-LSS correlation effects
  - ISW effect at large scale due to the time variation of the linear potentials in non EdS universe (large angular scales)
  - Thermal and kinetic SZ effects from clusters : probably the principal source of worries for accurate reconstructions the convergence maps

Conclusions

- The reconstruction methods for the lens fields are established on solid grounds although further numerical studies are needed *(see Amblard, Vale & White '04)*

- So far no detection of cross-correlation *(Hirata et al. '04)*

- Such methods open the way to tomographic exploration of the dark matter distribution of the Universe in conjunction with cosmic shear measurements.

- Looking forward to *Planck+CFHTLS (SNAP / JDEM)* data...